Evaluation of Types of Interactions in Subunit Association in *Bacillus subtilis* Adenylosuccinate Lyase†

Lushanti De Zoysa Ariyananda and Roberta F. Colman*

Department of Chemistry and Biochemistry, University of Delaware, Newark, Delaware 19716

Received July 16, 2007; Revised Manuscript Received December 19, 2007

ABSTRACT: Adenylosuccinate lyase (ASL) of *Bacillus subtilis* is a homotetramer in which three subunits contribute to each of four active sites. We sought to evaluate the types of interactions responsible for subunit association by studying the enzyme's oligomeric structure at low temperatures as compared to 25 °C, in the presence of KBr and after mutagenesis. Analytical ultracentrifugation data reveal that at 25 °C ASL is active and exists as 100% tetramer, while at 8 and 4 °C, as hydrophobic interactions are weakened, the catalytic activity decreases strikingly and the enzyme dissociates to a mixture of monomer–dimer–trimer, with small amounts of tetramer. In the presence of increasing concentrations of KBr (0.1–2.5 M), which disrupts electrostatic interactions, ASL is dissociated initially to monomer–dimer, with small amounts of trimer−tetramer, and then the monomer species predominates along with small amounts of trimer−tetramer. Very low enzymatic activity was found under these conditions. Accordingly, we postulate that electrostatic interactions are a major source of oligomeric stabilization of *B. subtilis* ASL. We selected for mutagenesis the closest charged residues (His^{299}/Glu^{239} and Arg^{167}/Asp^{217} pairs) located in the subunit interface that has the largest surface area. All of the mutants have low V_{max} values, high K_M values, and decreased molecular masses. We conclude that both hydrophobic and electrostatic interactions play roles in maintaining the ASL tetramer and this structure is essential for adenylosuccinate lyase activity.

Adenylosuccinate lyase (EC 4.3.2.2) catalyzes two reactions in the *de novo* synthesis of purines: the cleavage of adenylosuccinate (SAMP)[1] to AMP and fumarate and the conversion of 5-aminoimidazole-4-(*N*-succinylocarboxamide ribonucleotide) (SAICAR) to 5-aminoimidazole-4-carboxamide ribonucleotide (AICAR) and fumarate (*1*). The overall reaction is a β-elimination in which the β-H of the succinyl moiety of SAMP is abstracted by a general base and the leaving group (AMP) is protonated at either the *N*-1 or the *N*-6 position by a general acid (*1, 2*). Affinity labeling along with site-directed mutagenesis studies of the *Bacillus subtilis* enzyme has indicated that His^{68} and His^{141}, which are contributed by two different subunits, act as the general acid and base (*3–5*). Also, it has been shown that His^{89} (*6*), Lys^{268}, Glu^{275} (*7*), Asn^{276} (*8*), Gln^{212}, Asn^{270}, and Arg^{301} (*9*) are important for substrate binding and for catalysis.

ASL is a homotetramer (Figure 1-I) in which each subunit contains 431 amino acids and has a molecular mass of approximately 50 kDa. The enzyme has four active sites, and three subunits contribute amino acids to each active site (*7*). For example, in the circled active site shown in Figure 1-I, residues His^{141}, Glu^{275}, and His^{68} are supplied respectively by A, B, and C subunits. The homotetramer has three different types of subunit interface (Figure 1), and the interface between the A/C or B/D subunits has the largest contact area. Multimeric enzymes are held together by hydrophobic, electrostatic, and H-bonding interactions. The object of this study is to evaluate the types of interactions responsible for subunit association by studying the *B. subtilis* enzyme's oligomeric structure at low temperatures (8 and 4 °C) in the presence of KBr and after mutagenesis. A preliminary version of this study has been presented (*10*).

EXPERIMENTAL PROCEDURES

Materials. SAMP, HEPES, and imidazole were purchased from Sigma Chemical Co. Sephacryl S-200HR was purchased from Pharmacia. Bio-Rad dye concentrate was purchased from Bio-Rad Laboratories. All other reagents were purchased from Fisher and were of reagent grade. DNA sequencing primers and oligonucleotides for site-directed mutagenesis were obtained from Biosynthesis, Inc. The QuikChange site-directed mutagenesis kit was obtained from Stratagene, and the QIAprep spin miniprep kit was supplied by Qiagen.

Site-Directed Mutagenesis, Enzyme Expression, and Purification. The Stratagene QuikChange mutagenesis kit was used to introduce mutations to the pBHis plasmid (a gift from Dr. Jack E. Dixon, University of California, San Diego) that encodes adenylosuccinate lyase of *B. subtilis*. The oligonucleotides shown below and their complementary sequences were used to introduce the mutations into the cDNA: H299N,

† This work was supported by NIH Grant DK60504. The Beckman Optima XL-I analytical ultracentrifuge used in this study was obtained and supported by NIH 2P20 RR016472.

* To whom correspondence should be addressed. Phone: (302) 831-2973. Fax: (302) 831-6335. E-mail: rfcolman@udel.edu.

[1] Abbreviations: ASL, adenylosuccinate lyase; SAMP, adenylosuccinate; SAICAR, 5-aminoimidazole-4-(*N*-succinylocarboxamide ribonucleotide); AICAR, 5-aminoimidazole-4-carboxamide ribonucleotide; AMP, adenosine 5′-monophosphate; HEPES, *N*-(2-hydroxyethyl)piperazine-*N*′-ethanesulfonic acid; AUC, analytical ultracentrifugation; CD, circular dichroism; SDS−PAGE, sodium dodecyl sulfate−polyacrylamide gel electrophoresis; WT, wild type; SE, sedimentation equilibrium.

10.1021/bi701400c CCC: $40.75
Published on Web 02/01/2008

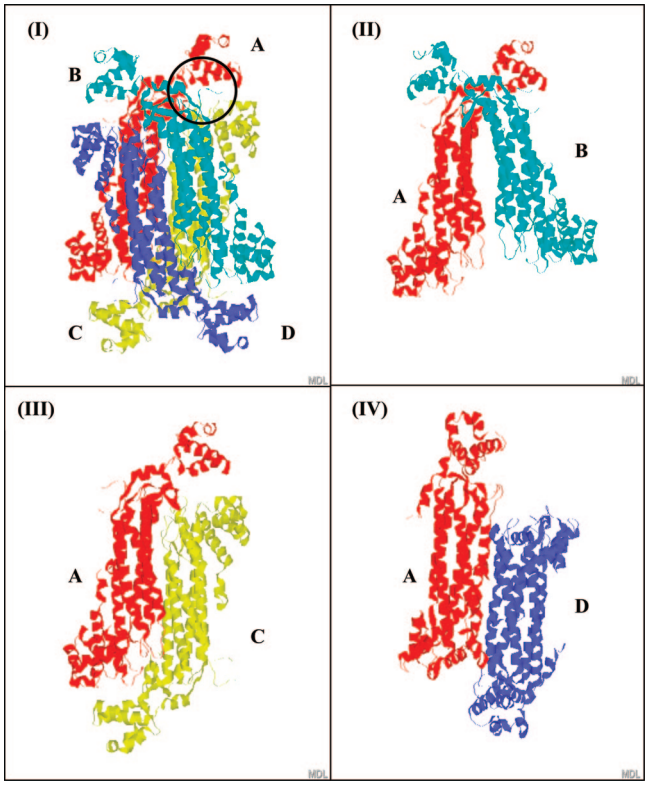

FIGURE 1: (I) Homology model of ASL of *B. subtilis* based upon the crystal structure of *Thermatoga maritima* ASL (*9*). Each individual subunit is color-coded. The location of one active site of four is shown by a circle. (II−IV) Three different types of subunit interface found within the ASL tetramer. The subunit interface between A and C (or the equivalent B and D) subunits has the largest contact area, whereas the subunit interface between A and B (or the equivalent C and D) subunits has the least contact area.

GTT CCA TTA TGG AAT GAG CGC GAT ATT TC; H299K, GTT CCA TTA TGG AAA GAG CGC GAT ATT TC; H299R, GTT CCA TTA TGG CGT GAG CGC GAT ATT TC; E239R, C GAG AAA TTC GCT GTG CGC ATC CGC G; E239Q, C GAG AAA TTC GCT GTG CAG ATC CGC G; E239M, C GAG AAA TTC GCT GTG ATG ATC CGC G; D217N, C CTT CAG CGT AAC CGC CAT GCT GAC; R167E, G AAA CGT AAT CTT GAG GAA TTC AAA CAA GC; and R167Q, G AAA CGT AAT CTT GAG CAG TTC AAA CAA GC. The cDNA was extracted and purified using the QIAprep spin miniprep kit. The mutations were confirmed by DNA sequencing, which was performed at the University of Delaware Center for Agriculture Biotechnology using an ABI Prism model 377 DNA sequencer (PE Biosystems).

The pBHis plasmid, which encodes a His_6 tag on the N-terminus of ASL, was expressed in *Escherichia coli* strain BL21(DE3). The wild-type (WT) and the mutant enzymes were purified to homogeneity using chromatography on Qiagen nickel nitrilotriacetic acid−agarose (*3, 11*). The purity of the enzymes was assessed by 12% polyacrylamide gels containing 0.1% sodium dodecyl sulfate. The protein concentration was determined by absorbance at 280 nm using $E_{280}^{1\%} = 10.6$ (*3*). After purification, the enzyme was aliquoted and stored in −80 °C in 20 mM KPO_4 buffer containing 20 mM KCl, pH 7.

Enzymatic Assays under Various Conditions. The activity of the preincubated WT or the mutants was measured continuously by assaying (over a 1 min period) at pH 7, 25 °C, in 50 mM HEPES buffer. The activity was measured from the decrease in absorbance at 282 nm as 60 μM SAMP is converted to AMP and fumarate (standard assay). The difference extinction coefficient of 10000 M^{-1} cm^{-1} between SAMP and AMP was used to calculate the specific activity, which was expressed in micromoles of substrate converted per minute per milligram of enzyme used (*12*). The assay was linear over the 1 min period.

The activity of the WT enzyme at low temperatures was monitored as follows: various concentrations (0.4, 0.2, and 0.08 mg/mL) of WT enzyme in 20 mM KPO_4 buffer, pH 7.0, containing 20 mM KCl were preincubated at 25 °C for 30 min. Then each sample was separately preincubated in water baths at 4 and 8 °C for ∼48 h. After the first 30 min of preincubation at 4 and 8 °C enzyme aliquots (16 μg in 40–200 μL) were periodically withdrawn and assayed for 1 min under standard assay conditions at 25 °C by adding the aliquot to a 1 mL assay mixture.

Although the effects of temperature on enzyme activity are reversible, this is a slow process, requiring 30 min for full reactivation after preincubation at low temperatures. The assay is linear over the first minute and reflects the enzyme activity at low temperatures. We have previously shown, when studying the effects of protein concentration on the activity of *B. subtilis* ASL (*8*), that the equilibrium between the dimer and tetramer is established slowly relative to the time of the assay.

The effect of KBr on the activity of the WT enzyme was studied as follows: WT enzyme (∼0.4 mg/mL) in 20 mM KPO_4 buffer, pH 7.0, containing various concentrations of KBr (0.1−2.5 M) was separately incubated at 25 °C for ∼48 h. Enzyme aliquots (20 μL) were periodically assayed for 1 min under standard assay conditions at 25 °C by adding the aliquot to a 1 mL assay mixture; the assay was linear over 1 min. For the control assays, WT enzyme of 0.4 mg/mL in 20 mM KPO_4 buffer, pH 7.0, in the absence of KBr, was preincubated at 25 °C for 30 min. In order to correct for the effect of "carried over" KBr on the assays, this WT enzyme (20 μL) was assayed after adding 20 μL of 20 mM KPO_4, pH 7.0, containing various concentrations of KBr (0.1−2.5 M) directly to the standard assay mixture.

The activities of the mutant enzymes were measured by preincubating the enzymes (∼0.4 mg/mL) in 20 mM KPO_4 buffer, pH 7.0, containing KCl for 30 min at 25 °C and then assaying for 1 min under standard assay conditions. The K_M values were determined by varying the SAMP concentrations (1−250 μM). Since SAMP has a high absorbance at 282 nm at concentrations >100 μM, at higher substrate concentrations the assays were conducted at 290 nm using a difference extinction coefficient of 4050 M^{-1} cm^{-1} (*8*). The data were analyzed by Michaelis–Menten plots with SE estimates obtained from the SigmaPlot software (SPSS Inc., Chicago, IL).

Circular Dichroism Spectroscopy. The secondary structure of the WT and mutant enzymes was assessed using CD spectroscopy. Ellipticity was measured on a Jasco J-710 spectropolarimeter from 200 to 250 nm, in 0.2 nm increments using a 0.1 cm cylindrical quartz cuvette. The samples were scanned five times and averaged, and the background from the buffer (20 mM KPO_4 and 20 mM KCl, pH 7) was subtracted. Final protein concentrations were measured using

the Bio-Rad protein assay, which is based on the method of Bradford (*13*). The mean molar residue ellipticity [θ] (deg cm^2 dmol^{-1}) was calculated from the equation [θ] = θ/10*nCl*, where θ is the measured ellipticity in millidegrees, *C* is the molar concentration of enzyme subunits, *l* is the path length in centimeters, and *n* is the number of residues per subunit (437, including the His_6 tag).

In order to measure ellipticity of the WT enzyme at various temperatures (4, 8, and 25 °C) enzyme samples of 0.4 mg/mL were preincubated at 25 °C for 30 min, after which they were incubated separately at 4 and 8 °C for ~2 h prior to acquiring CD data. The quartz cuvette was thermostated at the desired temperature while acquiring CD data.

Mutant enzyme samples of 0.4 mg/mL in 20 mM KPO_4 containing 20 mM KCl, pH 7, were incubated at 25 °C for 30 min prior to acquiring CD data. The ellipticity of the samples was measured at 25 °C.

Molecular Mass Determination Using AUC. Sedimentation equilibrium (SE) experiments of the WT and mutant enzymes were conducted using a Beckman Coulter ProteomLab XL-I analytical ultracentrifuge equipped with an An-60Ti analytical rotor. Samples were centrifuged at a certain speed, and after equilibrium was reached (~17 h), stepwise radial scans were performed at a particular wavelength, using a step size of 0.001 cm (*14*). Initially, equilibrium time was confirmed by scanning at 5 h intervals. Data were analyzed using the SEDPHAT program (*15*). In all of the cases (except for WT enzyme at 25 °C and in the absence of KBr) the experimental data were globally fitted, assuming that there is a continuous distribution of noninteracting species, to all the possible theoretical models of an oligomer in equilibrium with species of lower molecular mass. The models that gave best fits were chosen as the representative of that sample. The density of the buffers was calculated using the SEDNTERP program (*16*).

SE runs were performed for WT enzyme samples of 0.4, 0.2, and 0.08 mg/mL in 20 mM KPO_4 buffer, pH 7.0, containing 20 mM KCl separately at 4, 8, and 25 °C, by centrifuging them at 9K and 11K rpm. After equilibrium (~17 h) was reached, stepwise radial scans were performed for 0.4, 0.2, and 0.08 mg/mL samples at 280, 240, and 235 nm, respectively.

SE runs of the WT enzyme samples in the presence of KBr were done as follows: WT enzyme samples of 0.4 mg/mL in 20 mM KPO_4 buffer, pH 7.0, containing various concentrations of KBr (0.1−2.5 M) were prepared. They were centrifuged at 9K and 11K rpm and at 25 °C. After equilibrium was reached (~17 h), stepwise radial scans were performed at 280 nm.

The mutant and WT enzyme samples of 0.4 mg/mL in 20 mM KPO_4 buffer, pH 7.0, containing 20 mM KCl were incubated at 25 °C for 30 min. Sedimentation equilibrium experiments were performed at 25 °C using 8K and 10K rpm for His^{299} mutant enzymes, 8K and 9K rpm for Glu^{239} mutant enzymes, and 10K and 15K rpm for the Arg^{167}/Asp^{217} pair. After equilibrium was reached (~17 h), stepwise radial scans were performed at 280 nm.

Molecular Mass Determination of WT and Mutant Enzymes Using Gel Filtration Chromatography. A Sephacryl 200HR (1 × 92 cm) column was used, which was equilibrated in 20 mM KPO_4 buffer, pH 7.0, containing 20 mM KCl at room temperature. Protein samples of 3 mg/mL were loaded onto the column. Molecular mass standards from Amersham Biosciences were used to determine the molecular mass of WT and mutant enzymes.

Modeling of B. subtilis ASL Based on the Structure of T. maritima. Homology models of *B. subtilis* ASL have been constructed using as templates the structure of either the *T. maritima* enzyme crystallized at pH 4.5 (PDB 1c3c) or the structure of the same enzyme crystallized at pH 9.0 (PDB 1c3u) (*17*). Here we use the homology model of the *B. subtilis* based on the native *T. maritima* enzyme structure (PDB 1c3u) to study the mutations in the subunit interface (*9, 17*). The mutant enzymes were modeled by replacing the individual amino acids at positions 167, 217, 239, and 299 with the amino acids corresponding to the mutations made at each position. In all cases, the enzyme structure was energy minimized using the Discover 3.1 Insight II (2000) software package from Molecular Simulations, Inc., on a Silicon Graphics Indigo 2 work station.

Intersubunit contact area and the amount of hydrophobic and polar residues in the intersubunit contact area in the *T. maritima* enzyme structure (PDB 1c3c) were obtained by the use of the Protein Explorer program (free software by Erick Martz) (*18*). These results were compared to the homology model of the *B. subtilis* enzyme structure, which was based on the *T. maritima* enzyme structure.

RESULTS

Effect of Temperature on WT B. subtilis ASL. (A) Influence on Molecular Mass. We sought to evaluate the importance of hydrophobic interactions on the oligomeric structure of the enzyme. Since hydrophobic interactions are weakened as the temperature is decreased (*19–21*), the effect of cold temperatures on the oligomeric state of the enzyme was assessed using analytical ultracentrifugation (AUC). Three different protein concentrations were used to determine the molecular mass at 8 and 4 °C. Since the best fit models at 8 and 4 °C for the 0.4 and 0.2 mg/mL samples are very similar, only the results of 0.4 and 0.08 mg/mL are shown in Table 1. ASL is an oligomer of identical subunits of 50 kDa, and at 25 °C the enzyme exists purely as a tetramer. At low temperatures, hydrophobic interactions are weakened (*19–21*), and it is evident that at 8 and 4 °C the tetrameric enzyme dissociates into a mixture of species with lower molecular masses.

The experimental AUC data at these temperatures were globally fitted to various theoretical models for an oligomer in equilibrium with species of lower molecular mass. Representative residuals, which illustrate the goodness of the fit for various models, are shown in Figure 2, and the results are summarized in Table 1. At 8 °C the following theoretical models fit equally well: monomer–dimer−tetramer and dimer–trimer−tetramer for the 0.4 mg/mL sample and monomer–dimer−tetramer and monomer−trimer−tetramer for the 0.08 mg/mL sample (Figure 2A,B). The best fit model at 4 °C independent of the protein concentration is the monomer–dimer−tetramer model (Figure 2C,D). All of these models indicate that, irrespective of the protein concentration, there is a discrete amount of tetramer (on average ~37% at 8 °C and ~13% at 4 °C) along with variable amounts of the monomer, dimer, or trimer species depending upon the protein concentration; clearly, the equilibria involving the

Table 1: Molecular Masses and Catalytic Activity of WT *B. subtilis* ASL after Incubation at Various Temperatures[a]

incubation temp (°C)	0.4 mg/mL sample				0.08 mg/mL sample			
	AUC data[b] [kDa (%)]			specific activity[c] (μmol min^{-1} mg^{-1})	AUC data[b] [kDa (%)]			specific activity[c] (μmol min^{-1} mg^{-1})
	tetramer	M−D−Tet	D−Tri−Tet		tetramer	M−D−Tet	D−Tri−Tet	
25	205 (100)			1.7 ± 0.1	192 (100)			1.4 ± 0.1
8		46 (8)	94 (60)	0.4 ± 0.1		50 (48)	55 (52)	0.3 ± 0.1
		105 (55)	144 (2)			101 (17)	153 (16)	
		217 (36)	216 (38)			208 (35)	210 (32)	
4		50 (81)		0.2 ± 0.1		49 (88)		0.2 ± 0.1
		102 (6)				101 (1)		
		212 (13)				199 (11)		

[a] The enzyme samples were preincubated separately at 25, 8, and 4 °C in 20 mM KPO_4 buffer, pH 7, containing 20 mM KCl. [b] The molecular mass of the enzyme samples was determined by AUC using 11K rpm at 25, 8, and 4 °C in 20 mM KPO_4 buffer, pH 7, containing 20 mM KCl. M = monomer, D = dimer, Tri = trimer, and Tet = tetramer, and the dash (−) is used to indicate that different species are in equilibrium. [c] The specific activities in every case were measured at 25 °C by addition of a 16.0 μg aliquot of enzyme to 1.0 mL of solution containing 50 mM HEPES buffer, pH 7, and 60 μM SAMP.

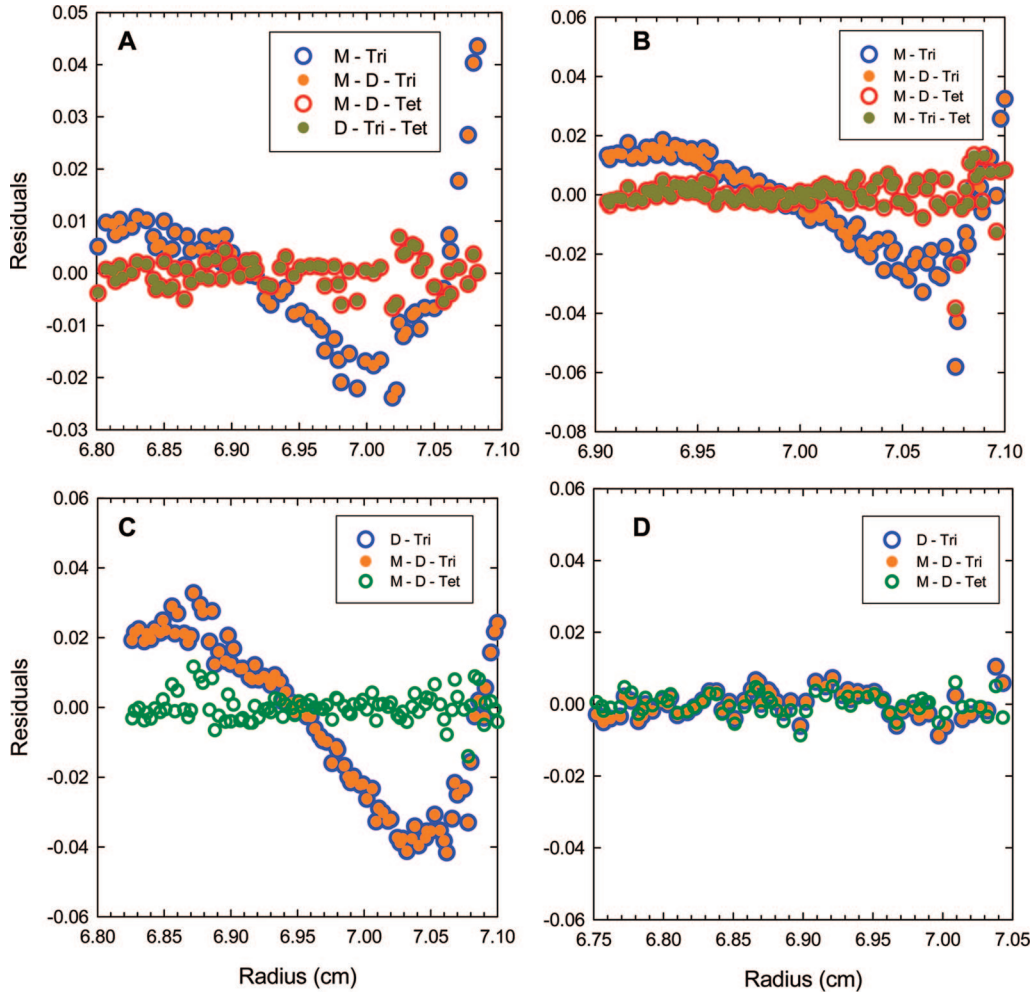

FIGURE 2: Representative experimental AUC residual data of the WT ASL enzyme at low temperatures. M = monomer, D = dimer, Tri = trimer, and Tet = tetramer. (A) Residuals for various models at 8 °C for the 0.4 mg/mL sample; the best fit models are M−D−Tet and D−Tri−Tet. (B) Residuals for various models for the 0.08 mg/mL sample at 8 °C; the M−D−Tet and M−Tri−Tet theoretical models gave the best fits. The M−Tri and M−D−Tri theoretical models on (A) and (B) are representatives of the models that gave a poor fit. (C, D) Residuals for various models for the 0.4 and 0.08 mg/mL samples at 4 °C are shown, respectively. The M−D−Tet theoretical model correlates well with the experimental data whereas D−Tri and M−D−Tri theoretical models are examples that had poor fits. For the 0.08 mg/mL sample (graph D) all of the three state models gave the M−D−Tet molecular masses.

lower molecular mass species cannot be distinguished. According to the best fit models at 8 °C, the 0.4 mg/mL sample is composed of predominantly dimer (~58%) along with ~37% tetramer and ~5% monomer−trimer (Table 1 and Figure 2A), whereas the 0.08 mg/mL sample is constituted predominantly of monomer (~50%) along with ~35% tetramer and ~15% dimer–trimer (Table 1 and Figure 2B). In contrast, at 4 °C the best fit model for 0.4 and 0.08 mg/mL samples suggests that ~85% monomer is in equilibrium with ~12% tetramer and ~4% dimer (Table 1 and Figure 2C,D).

(B) Influence on Enzymatic Activity. Since there is a drastic change in the molecular mass as the temperature is decreased, we sought to assess the stability of the enzyme at lower temperatures as compared to 25 °C. The enzyme was preincubated for ~48 h at 25, 8, or 4 °C, and the specific

Table 2: Molecular Mass Data and Kinetic Parameters of WT *B. subtilis* ASL in the Presence of Various Concentrations of KBr at 25 °C

	AUC data[a] [kDa (%)]							exptl sample specific activity[b]	control sample specific activity[c]	fraction of activity due to incubation[d]
[KBr] (M)	tetramer	D−Tri−Tet	M−Tet	D−Tet	Tri−Tet	D−Tri	M−Tri	(μmol min^{-1} mg^{-1})	(μmol min^{-1} mg^{-1})	(%)
0	205 (100)							1.50 ± 0.05	1.50 ± 0.05	100
0.1		216 (35) 151 (10) 96 (55)						0.46 ± 0.14	1.35 ± 0.07	34
0.2			211 (38) 51 (62)	210 (37) 105 (63)	217 (39) 142 (61)			0.24 ± 0.18	1.26 ± 0.02	19
0.3			213 (37) 64 (63)	215 (37) 112 (63)	210 (35) 153 (65)			0.17 ± 0.13	1.21 ± 0.07	14
0.4			214 (37) 45 (63)	229 (34) 91 (64)	208 (35) 157 (65)			0.17 ± 0.16	1.05 ± 0.12	16
0.5			204 (35) 49 (65)	211 (36) 98 (64)	211 (35) 149 (65)			0.12 ± 0.02	0.79 ± 0.04	15
1.0			213 (37) 52 (63)	222 (36) 112 (64)	218 (25) 143 (75)			0.05 ± 0.01	0.56 ± 0.02	10
1.5			210 (35) 47 (65)	215 (31) 114 (69)	220 (21) 152 (79)			0.04 ± 0.01	0.48 ± 0.01	9
2.0			193 (7) 64 (93)	191 (10) 96 (90)		164 (5) 97 (95)		0.04 ± 0.01	0.36 ± 0.03	10
2.5			189 (8) 50 (92)				176 (5) 49 (95)	0.03 ± 0.01	0.30 ± 0.01	10

[a] The molecular mass of the enzyme was determined by AUC using 11K rpm at 25 °C in the presence of 20 mM KPO_4 buffer, pH 7, containing various concentrations of KBr. M = monomer, D = dimer, Tri = trimer, and Tet = tetramer, and the dash (−) is used to indicate that different species are in equilibrium. [b] The enzyme was separately preincubated at 25 °C in 20 mM KPO_4 buffer, pH 7, containing various concentrations of KBr. The activities were measured at 25 °C by addition of a 20 μL aliquot of enzyme to 1.0 mL of solution containing 50 mM HEPES buffer, pH 7, and 60 μM SAMP. [c] For the control experiment, enzyme was preincubated at 25 °C in 20 mM KPO_4 buffer, pH 7, in the absence of KBr; this control enzyme was assayed by addition of 20 μL of enzyme to 1.0 mL of solution containing 50 mM HEPES buffer, pH 7, and 60 μM SAMP, plus 20 μL of the buffer containing various concentrations of KBr. [d] The ratio of the exptl sample to the control sample × 100.

activity was determined by rapid addition to an assay solution at 25 °C, yielding linear rates over a 1 min period. The activity decreases within the first half hour of preincubation at the lower temperatures, after which it remains the same during the rest of the time period. The average specific activities of 0.4 and 0.08 mg/mL samples for the time period (0.5−48 h) are shown in Table 1. The specific activities obtained for the 0.2 mg/mL sample were similar to that of 0.4 mg/mL sample. The results show that at 8 and 4 °C the activity decreases to about 23% and 10%, respectively, of the initial value at 25 °C. After preincubation at these low temperatures, these specific activities do not vary appreciably with the concentration of the enzyme.

When the enzyme samples, which had first been incubated at 8 and 4 °C, were incubated at 25 °C, they slowly regained their full activity, implying that the dissociation observed at low temperatures is reversible. However, the enzyme with decreased activity at low temperatures had to be incubated at 25 °C for ∼30 min in order to regain its full activity. Since the standard assays were measured for only 1 min, it is evident that the linear rates reflect the activity at low temperature (see Experimental Procedures). Hence, the striking decrease in activity as the temperature is lowered is largely due to the loss of the tetrameric structure of the enzyme. These results demonstrate that ASL has to be in the tetrameric form to be fully active.

(C) Influence on Secondary Structure. Since there is a marked decrease in activity and in weight average molecular mass at low temperatures, circular dichroism (CD) was used to ascertain whether there is any change in the secondary structure of the protein under the same conditions. The CD spectra obtained at 4 and 8 °C are superimposable on that at 25 °C (data not shown). The near identity of the three spectra indicates that there is no appreciable change in the secondary structure when the temperature is varied. ASL exhibits minima at 208 and 222 nm, which is typical of proteins containing appreciable amounts of α-helix (*5*).

Effect of KBr on WT B. subtilis ASL. (A) Influence on Molecular Mass at 25 °C. Monovalent anions have been used to disrupt the electrostatic interactions between subunits of multimeric proteins (*19, 22, 23*). KBr was selected for this study since, in accordance with the Hofmeister series of monovalent anions, bromide is an effective protein destabilizing and dissociating agent (*19*). To evaluate the effect of various concentrations of KBr on the oligomeric state of the enzyme, AUC was used. The experimental AUC data were globally fitted to all possible theoretical models for an oligomer in equilibrium with species of lower molecular masses. The results are summarized in Table 2, and representative residuals for various models are shown in Figure 3.

At 0.1−0.5 M KBr, the models indicate that there is a discrete amount of tetramer (on average ∼36%) and the remaining 64% exist as monomer, dimer, or trimer; therefore, the equilibria involving the lower molecular mass species cannot be distinguished. The best fit model at 0.1 M KBr is the dimer–trimer−tetramer, and at KBr concentrations ≥0.2 M only the two species models fit well. According to the models at 0.2−0.5 M KBr, the enzyme sample is composed predominantly of monomer–dimer–trimer (∼63%). As the KBr concentration is increased to 1.5 M, the amount of tetramer decreases and the amount of lower molecular mass species increases. Upon further increment of the KBr concentration to 2.0 M, WT ASL tends to dissociate predominantly to monomer–dimer (∼90%) along with ∼10% tetramer−trimer (Table 2). At 2.5 M KBr, the monomeric species predominates (∼97%) along with ∼3% tetramer−trimer. These results indicate the importance of electrostatic forces in maintaining the stability of the tetramer.

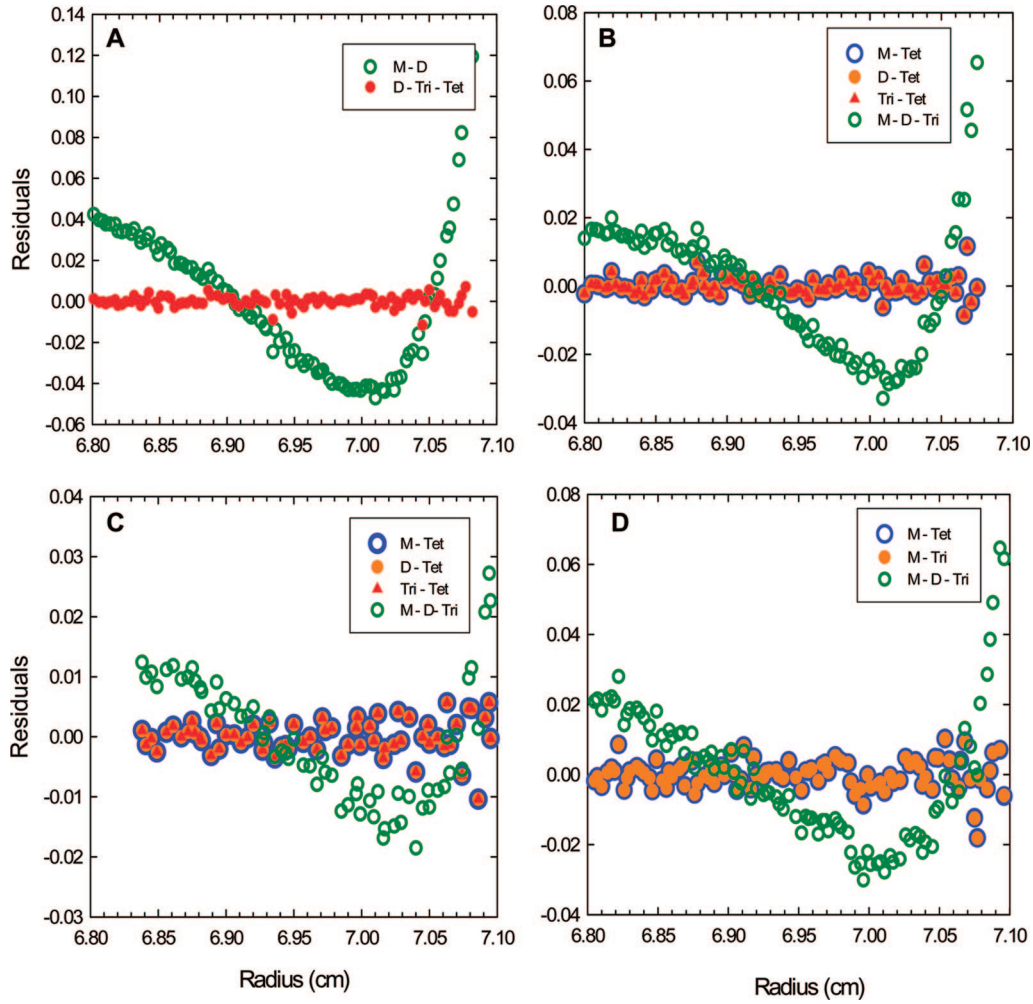

FIGURE 3: Representative experimental AUC data of the WT ASL enzyme in the presence of various KBr concentrations. (A) Residuals for various models for the enzyme in the presence of 0.1 M KBr; the best fit model is the D−Tri−Tet model. (B, C) Residuals for various models for the enzyme in the presence of 0.5 and 1.5 M KBr, respectively. The M−Tet, D−Tet, and Tri−Tet theoretical models superimpose on the experimental data. (D) Residuals for various models for the enzyme in the presence of 2.5 M KBr; the M−Tet and M−Tri theoretical models gave the best fits. The theoretical models that had poor fits are represented by the M−D model in (A) and the M−D−Tri model in (B)−(D).

(B) Influence on Enzymatic Activity. It is evident that, in the presence of KBr, WT ASL enzyme dissociates into different species. Therefore, in order to assess the stability, WT ASL was incubated at pH 7 and 25 °C, and the activity was monitored for ∼48 h. These results were averaged and are shown in Table 2. In the presence of 0.1, 0.2−0.5, and 1.0−2.5 M KBr the enzyme activity decreases to ∼31%, ∼16−8%, and ∼3−1%, respectively, of the initial activity without KBr.

This loss of activity could be entirely due to disruption of electrostatic interactions at the subunit interfaces during preincubation of the enzyme in the presence of various concentrations of KBr. Alternatively, KBr might adversely affect the assay. To distinguish between the effects, the enzyme was incubated at 25 °C in the absence of KBr, and its activity was measured by adding appropriate amounts of KBr directly to the assay mixture (to yield the same "carried over" concentration of KBr as in the samples of Table 2, column 4); the results of this *control* experiment are shown in Table 2, column 5. From 0.1 to 0.4 M and from 0.5 to 2.5 M KBr the control specific activity is ∼90−70% and ∼53−20%, respectively, of the initial activity without KBr. The results of the control experiment indicate that there is a decrease in activity as the carried over KBr concentration is increased.

The ratio of the specific activity of the experimental sample to that of the control sample gives the fraction of activity due to the preincubation of ASL in the KBr solution (Table 2, last column). Thus, at 0.1, 0.2−0.5, and 1.0−2.5 M KBr the actual specific activity due to preincubation is 34%, ∼19−15%, and ∼10%, respectively, of the corresponding control specific activity (Table 2, column 6).

Search by Mutagenesis for the Key Electrostatic Interactions at the A/C Subunit Interface. (A) Expression and Purity of the B. subtilis ASL Mutants. Since the electrostatic forces appear to make a major contribution toward stabilizing the subunits, we sought to identify the closest polar amino acid residues located in the A/C subunit interface (Figure 1-III). As shown in Figure 1 the tetrameric enzyme has three different interfaces; based on analysis of the intersubunit surface area, the interface between the A/C or B/D subunits has the largest contact area. For each potential electrostatic or H-bonding interaction, mutagenesis could then be used to evaluate its contribution to oligomeric structure. Some of

the human mutations (R194C, K246E, and R452P) that occur in ASL-deficient patients appear to be in the subunit interface that has the largest surface area (*24–26*). Furthermore, these mutations produce unstable enzymes. Therefore, we postulated that the subunit interface with the largest contact area might be an important contributor toward the stability of the *B. subtilis* ASL tetramer as well and any perturbation of the polar residues in this subunit interface of *B. subtilis* ASL could result in destabilized enzyme. The amino acid pairs selected as targets for mutagenesis were the His^{299}/Glu^{239} pair (2.93 Å apart) and the Arg^{167}/Asp^{217} pair (3.05 Å apart), as shown in Figures 4-I and 5-I, respectively. These pairs are sufficiently close to form a salt bridge or H-bond.

Some mutations were introduced to remove the charge (as in E239Q, E239M, R167Q, or D217N), while maintaining an amino acid side chain of similar size. Other mutations were chosen to reverse the charge at a particular position (as in E239R and R167E) and introduce electrostatic repulsion. The His^{299} residue might act as a positively charged residue, or it might be neutral and participate in H-bonding. To test these possibilities, His was mutated to Lys and Arg in order to maintain its potential positive charge; although the replacements are somewhat larger than His, H299K and H299R might behave similarly to the wild-type enzyme if His^{299} acts as a positively charged species. Alternatively, if His^{299} functions in its neutral form, it may be better replaced by Asn. All of the mutants were purified to homogeneity, and the purity was assessed using SDS−PAGE, as represented in Figure 6. Each enzyme exhibited a single subunit band with the expected subunit molecular weight of about 50000.

(B) Molecular Masses of the B. subtilis ASL His^{299} *and* Glu^{239} *Mutants.* The effect of these interface subunit mutations on the oligomeric state of the enzyme was assessed using AUC. A constant concentration of 0.4 mg/mL was used for all of the mutants of the His^{299}/Glu^{239} pair, and centrifugation was done at two different speeds. Since the experimental AUC data of both the speeds correlated equally well with the same models, only the AUC results at one speed are summarized in Table 3.

For the His^{299} mutants, the best fit models that describe the equilibrium mixture are the monomer−tetramer, monomer−trimer, and dimer–tetramer, where there is ∼85% of monomer–dimer and ∼15% of tetramer−trimer. None of the *three* species models had good fits, suggesting that the interchanging of tetramer to trimer or monomer to dimer could be very rapid, so that the three species cannot be distinguished.

All of the Glu^{239} mutant enzymes had good fits with monomer−tetramer, dimer−tetramer, or trimer−tetramer equilibria. These models suggest that the majority of the E239Q mutant enzyme exists as lower molecular mass species (∼70%) which could be either monomer, dimer, or trimer, with ∼30% tetramer, while E239M and E239R mutant enzymes exist predominantly of a mixture of monomer–dimer (∼96%) along with small amounts of tetramer (∼4%). It is evident that perturbing His^{299} or Glu^{239} produces greatly destabilized enzyme of lower than normal molecular mass; therefore, this interaction is important for maintaining the tetrameric structure of the enzyme.

As an alternative, the distribution of oligomeric species present in solutions of each mutant was evaluated using gel

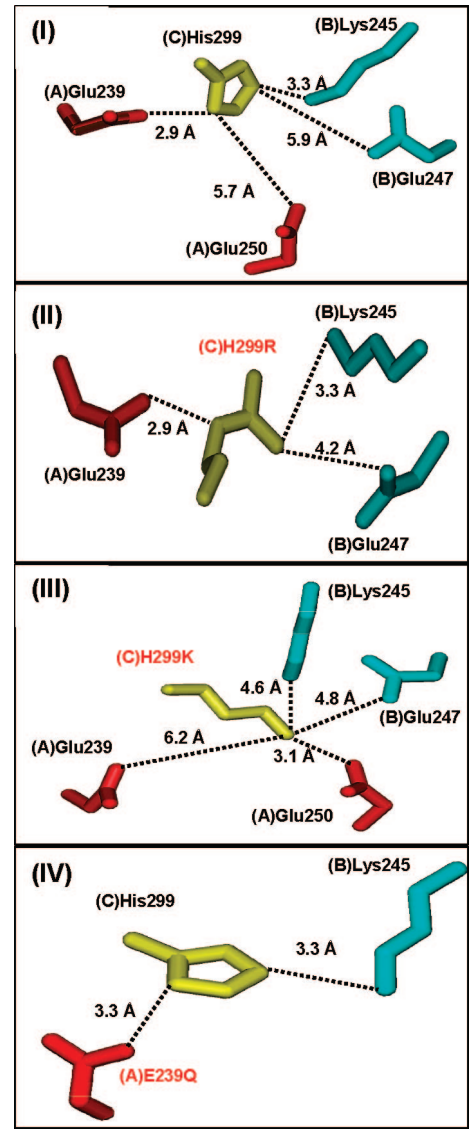

FIGURE 4: (I) The His^{299}/Glu^{239} pair located in the A/C subunit interface (which has the largest contact area) that is selected as target sites for mutagenesis and the residues in close proximity. Energy-minimized models of H299R, H299K, and E239Q are shown in (II), (III), and (IV), respectively. The color of each residue corresponds to the color scheme of the ASL tetramer.

filtration chromatography. Sample elution profiles of His^{299} and Glu^{239} mutants are shown in Figure 7A,B, and the results are summarized in Table 3. The elution profiles of the His^{299} mutants (Figure 7A) show a maximum at ∼160 kDa (closer to trimer mass), but the elution profiles span the tetramer region to the monomer region, implying that these mutant enzymes exist as a mixture of species. Since the AUC data suggest that there is a rapid interchange between tetramer and trimer or monomer and dimer of the His^{299} mutant enzymes, they are not separable. The average molecular masses from gel filtration (∼160 kDa) correlate well with the apparent molecular masses from AUC.

On the other hand, the elution profiles of Glu^{239} mutants (Figure 7B) show that these mutants have species with various molecular masses. The E239Q mutant enzyme has a maximum at ∼160 kDa; however, the elution profile is distributed over a wide range of molecular masses, indicating that the enzyme may be a mixture of monomer, dimer, trimer, and soluble aggregates. The E239R has a major peak at ∼131

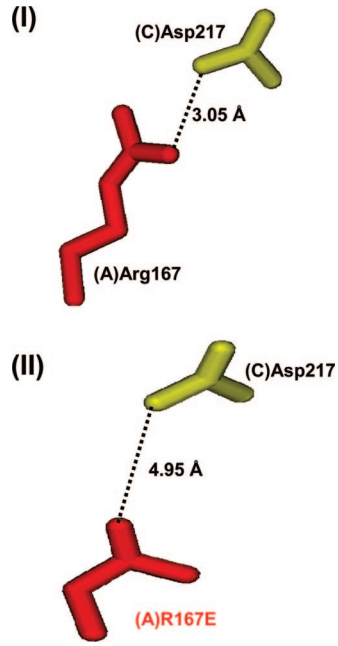

FIGURE 5: (I) The Arg^{167}/Asp^{217} pair located in the A/C subunit interface (which has the largest contact area) that was selected as target sites for mutagenesis. (II) Energy-minimized model of R167E. The color of each residue corresponds to the color scheme of the ASL tetramer.

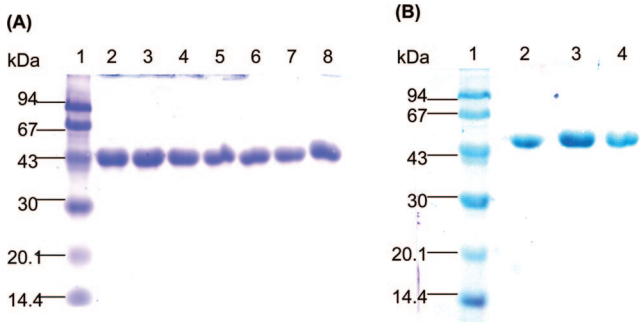

FIGURE 6: SDS−PAGE of representative purified enzymes. The protein(s) in each lane is (are) as follows: (A) lane 1, protein standards; lane 2, WT; lane 3, H299R; lane 4, H299K; lane 5, H299N; lane 6, E239R; lane 7, E239M; lane 8, E239Q; (B) lane 1, protein standards; lane 2, WT; lane 3, D217N; lane 4, R167Q.

kDa and a shoulder at 59 kDa, indicating that it is predominantly a mixture of monomer and dimer. Similarly, E239 M has a major peak at ~131 kDa, which broadens toward the monomer region, suggesting that it exists predominantly as a dimer with small amounts of monomer. These average molecular masses from gel filtration are in reasonable agreement with the apparent molecular masses from AUC.

(C) Kinetics of the B. subtilis ASL His^{299} and Glu^{239} Mutants. All of the mutant enzymes of the His^{299}/Glu^{239} pair had measurable catalytic activity and could be characterized kinetically. The data at pH 7.0 in the direction of AMP formation for the mutants of the His^{299}/Glu^{239} pair are shown in Table 3. Kinetic data for all of the mutant enzymes obeyed the simple Michaelis–Menten equation; the double reciprocal plots were linear over a wide range of substrate concentration, suggesting that there are no quaternary isoforms that are active except the tetramer form. Furthermore, in order to get measurable rates under standard assay conditions, a very high protein concentration (8 mg/mL) had to be used. Also, no time-dependent increase in specific activity was observed for any of the mutant enzymes, which indicates that there is no substrate-mediated equilibrium shift toward tetramer.

Against the possibility that His^{299} functions as a positively charged species are the observations that the V_{max} of H299K and H299R mutants are only ~1% that of the WT enzyme, while the V_{max} of the neutral substitution, H299N, is ~3.2% that of WT. Furthermore, the values of K_M for SAMP of *all* the His^{299} mutants are 10−15-fold higher than that of the WT (Table 3). These results suggest that His^{299} is not positively charged in its active form; rather, the unprotonated form of His^{299} is likely to be needed for ASL to function properly.

The V_{max} values for all of the Glu^{239} mutants are ~1−3% that of the wild type, while the K_M values of these mutants are 3−10-fold higher than that of the WT (Table 3). These results indicate that a carboxylate group at position 239 is essential for effective functioning of ASL.

(D) Molecular Masses of the B. subtilis ASL Arg^{167} and Asp^{217} Mutants. AUC was used to assess the effect of these interface subunit mutations on the oligomeric state of the enzyme. A constant concentration of 0.4 mg/mL was used for all of the mutants of the Arg^{167}/Asp^{217} pair, and each experiment was carried out at 10K and 15K rpm. At both speeds similar results were obtained from the best fit models; hence, only the data at 10K rpm are represented in Table 4. On the basis of the best fit models, R167Q and D217N mutant enzymes consist predominantly of a mixture of monomer–dimer (~95%) along with small amounts of soluble aggregates. The molecular mass of the soluble aggregates of R167Q is ~405 kDa whereas for D217N it is ~275 kDa. For the R167E mutant enzyme, the best fit model is the monomer–dimer model, which indicates that there is no tetramer present. It is clear that these mutations have greatly facilitated the dissociation of the tetrameric ASL into monomeric and dimeric species rather than trimeric species.

To evaluate the distribution of oligomeric species present in solutions of each mutant, we used gel filtration chromatography. Sample elution profiles of mutants of the Arg^{167}/Asp^{217} pair are shown in Figure 7C, and the results are summarized in Table 4. The elution profiles of mutants of the Arg^{167}/Asp^{217} pair show that solutions of these mutants contain species with a very wide range of molecular masses (Figure 7C) which correlate well with AUC data. Both R167E and R167Q mutants are a mixture of soluble aggregates with higher molecular masses (354 kDa), dimeric species (89 kDa), and monomeric species (~32 kDa). In contrast, the elution profile of D217N shows that it exists predominantly in dimeric form, with smaller amounts of monomeric species.

(E) Kinetics of the B. subtilis ASL Arg^{167} and Asp^{217} Mutants. The mutant enzymes of this pair, except R167E, had measurable catalytic activity and could be characterized kinetically. The data at pH 7.0 in the direction of AMP formation for the mutants of the Arg^{167}/Asp^{217} pair are shown in Table 4. The V_{max} values for R167Q and D217N are only ~1% that of the WT enzyme, and the R167Q has a K_M value for SAMP that is ~5 times that of WT. The R167E mutant enzyme, which is a charge reversal mutant, precipitated soon after purification, and the supernatant had no measurable activity. This observation indicates that the extent of repulsion is greater in this charge reversal mutant than in E239R,

Table 3: Molecular Mass Data and Kinetic Parameters of the *B. subtilis* ASL Mutants of the His299/Glu239 Pair

	AUC data[a] [kDa (%)]					gel filtration data[b]	$V_{max} \pm$ SE[c]	$K_M \pm$ SE[c]
enzyme	tetramer	M−Tet	M−Tri	D−Tet	Tri−Tet	(kDa)	(μmol min^{-1} mg^{-1})	(μM)
WT	205 (100)					216	1.56 ± 0.19	2.6 ± 0.4
H299N		225 (15)	157 (10)	240 (13)		160	0.05 ± 0.01	25.6 ± 4.7
		52 (85)	57 (90)	80 (87)				
H299K		278 (19)	152 (15)	241 (17)		160	0.02 ± 0.01	36.3 ± 2.4
		58 (81)	55 (85)	106 (83)				
H299R		265 (18)	165 (15)	350 (10)		160	0.02 ± 0.01	40.7 ± 1.5
		66 (82)	55 (85)	113 (90)				
E239Q		250 (33)		220 (35)	235 (20)	160	0.01 ± 0.01	7.6 ± 0.9
		53 (67)		106 (65)	153 (80)			
E239M		236 (8)		240 (4)		131	0.01 ± 0.01	30.0 ± 2.3
		52 (92)		97 (96)				
E239R		230 (3)		245 (5)		131	0.06 ± 0.01	25.7 ± 3.5
		53 (97)		99 (95)		59[d]		

[a] The molecular mass by AUC was measured at 25 °C in 20 mM KPO_4 buffer, pH 7, containing 20 mM KCl using 10K rpm for the His299 mutants and 9K rpm for the Glu239 mutants. M = monomer, D = dimer, Tri = trimer, and Tet = tetramer, and the dash (−) is used to indicate that different species are in equilibrium. [b] The molecular mass by gel filtration was done at 25 °C using a Sephacryl S-200 column equilibrated with 20 mM KPO_4 buffer, pH 7, containing 20 mM KCl. [c] The K_M and V_{max} values were determined by varying the concentration of SAMP and fitting the data to the Michaelis–Menten equation using SigmaPlot. The values are shown along with their standard errors. [d] Shoulder.

leading to a greater destabilization of the protein. The SAMP K_M value of D217N is about 16 times that of the WT enzyme.

(F) Circular Dichroism Spectroscopy of the B. subtilis ASL Mutants. CD spectroscopy was used to investigate any changes in the secondary structure of these mutants. As measured at a constant concentration of 0.4 mg/mL, the CD spectra of all of the mutants and WT enzyme exhibit minima at 208 and 222 nm, which is typical of proteins containing appreciable amounts of α-helix. The CD spectra of all of the His^{299} mutants are superimposable with that of WT, indicating that there are no major changes in the secondary structure of the protein.

The CD spectra of the Glu^{239} mutants exhibit small differences from that of WT (data not shown). The molar residue ellipticity at 208 nm for E239M and E239Q mutants is a little more negative than that of WT, implying that those mutants are slightly more α-helical in nature than the WT, while the E239R mutant has slightly lower molar residue ellipticity values. Moreover, the shapes of the CD curves of the mutants are distinguishable from that of the WT enzyme, with ratios of $\theta_{222}/\theta_{208}$ of 1.04 as compared to 1.13 for the WT enzyme.

The CD spectra of the mutants of the Arg^{167}/Asp^{217} pair have only minor changes. According to the CD spectrum of R167Q, it has slightly more α-helical character than that of WT, whereas the CD spectra of R167E, D217N, and WT are superimposable.

DISCUSSION

Adenylosuccinate lyase of *B. subtilis* is a homotetramer of ∼200 kDa at 25 °C; therefore, it has three different types of subunit interface (Figure 1). The subunits are held together by hydrophobic, electrostatic, and H-bonding interactions. Perturbation of any of these interactions can lead to a change in the oligomeric structure and the activity of ASL. In this study we have evaluated the contribution of these interactions to the stability of the tetramer.

At lower temperatures the secondary structure of WT ASL is unchanged, but we observed ∼90% loss of activity. As the temperature is decreased, hydrophobic interactions are weakened (*20, 21*) and the enzyme dissociates to smaller molecular mass species. However, at 8 and 4 °C, ∼35% and ∼13%, respectively, of the total enzyme exist purely as a tetramer irrespective of the protein concentration. At 8 °C, either the monomer or dimer species predominates depending on the protein concentration, along with small amounts of trimer and tetramer, whereas at 4 °C, the monomer species predominates independent of the protein concentration, along with small amounts of dimer and tetramer. If the trimer were active, one would expect different activities at 8 and 4 °C for the 0.08 mg/mL enzyme sample, but we observe very similar activities at these temperatures. Therefore, the residual activity appears to be attributable to the amount of tetramer present, and the loss of activity at low temperatures is due to the decreased amounts of tetramer. These results lead to the conclusion that even though the active site is composed of three subunits (*7*), the tetramer form has to be maintained for the enzyme to be fully active and the hydrophobic interactions in the subunit interface contribute to the stability of the tetramer.

At pH 7, we used a range of KBr concentrations (0.1−2.5 M) to disrupt the electrostatic interactions in the WT enzyme. Overall, as the KBr concentration is increased, the amount of tetramer decreases and lower molecular mass species increase. At the low concentrations of KBr (0.1−0.4 M), the WT ASL enzyme has a discrete amount of tetramer (∼35%), which is similar to that at 8 °C, and a mixture of monomer–dimer–trimer. Furthermore, the experimental specific activities at these KBr concentrations are within the range of 0.2−0.4 μmol min^{-1} mg^{-1}, which are in a reasonable agreement with that at 8 °C. These findings support the postulate that the activity is due to the amount of tetramer present and the lower molecular mass species are inactive. Further increase of KBr concentration (1.0−2.5 M) promotes the dissociation of the tetrameric enzyme first to monomer–dimer and then mainly to monomer; hence, there is no discrete amount of tetramer present. The experimental specific activity is always below the 0.1 μmol min^{-1} mg^{-1} level. These results lead to conclusion that any perturbation of the tetrameric structure drastically decreases the activity of the enzyme.

Monovalent anions such as halides are known to disrupt the electrostatic interactions in a protein, and their arrangement in increasing order of destabilizing a protein (F^- <

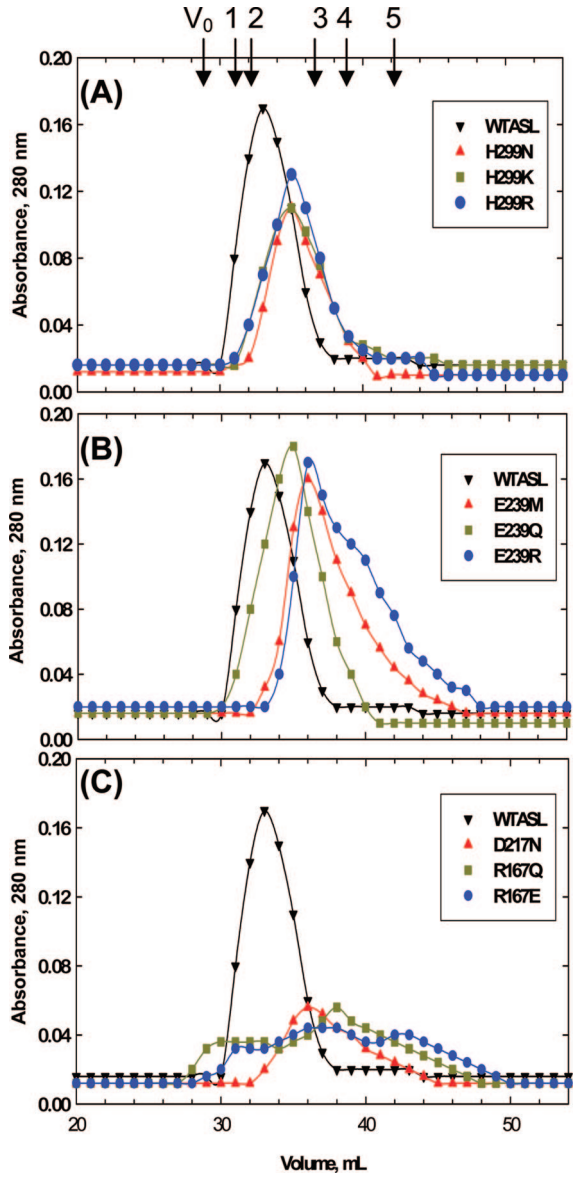

FIGURE 7: Gel filtration elution profiles of WT and mutant enzymes at 25 °C. These elution profiles were obtained by applying 1 mL of each protein (~3 mg/mL) to a Sephacryl 200HR column (1 × 92 cm) equilibrated with 20 mM KPO_4 buffer, pH 7, containing 20 mM KCl. The molecular mass standards used are as follows: V_0, blue dextran; 1, ferritin, 440 kDa; 2, catalase, 232 kDa; 3, yeast alcohol dehydrogenase, 141 kDa; 4, albumin, 67 kDa; 5, ovalbumin, 43 kDa. The elution profiles of His^{299}, Glu^{239}, and Arg^{167}/Asp^{217} mutants are shown in (A), (B), and (C), respectively.

$Cl^- < Br^- < I^-$) is called the Hofmeister series. Such monovalent Hofmeister anions could destabilize a protein using one or more of the following mechanisms: Hofmeister effect, Debye screening effect, and anion binding mechanism (*22*). In the Hofmeister effect, the anions have favorable interactions with the peptide groups of the protein and unfavorable interactions with the nonpolar side chains of the protein. According to their net interactions, the extent of destabilizing a protein by these anions would be different (*22*). On the other hand, in the Debye screening effect, the mobile anions in an aqueous solution are expected to reduce the strength of any favorable and repulsive interactions within a protein, whereas anion binding should reduce the strength only of the unfavorable interactions among positively charged residues within the protein (*22*). The screening efficiency of a halide generally agrees with its position in the Hofmeister series (*23*); therefore, the Br^- anion should be an efficient protein destabilizing agent. If only unfavorable interactions were screened as the Br^- concentration is increased, we would expect the tetrameric form of the enzyme to be more stable at higher Br^- concentrations. Dissociation of the ASL enzyme into different species in the presence of different KBr concentrations indicates that this destabilization occurs either by the Hofmeister effect or by Debye screening rather than by anion binding. The Br^- probably screens favorable interactions between positive and negative charges on different subunits, thereby facilitating the dissociation of subunits.

From our results, it is evident that at 8 and 4 °C the enzyme dissociates into a mixture of monomer–dimer–trimer−tetramer and monomer–dimer−tetramer, respectively, and the dissociation is reversible. On the other hand, in the presence of increasing concentrations of KBr, the enzyme dissociates initially to a mixture of monomer–dimer–trimer−tetramer and then predominantly to monomer with very small amounts of tetramer−trimer, and this effect is irreversible. These findings suggest that the electrostatic interactions at the subunit interface could have a greater effect than the hydrophobic interactions on the stability of the ASL tetramer. Accordingly, we selected for mutagenesis two pairs of polar amino acid residues at the subunit interface; in one case, the negatively charged Asp interacts with the positively charged Arg (Arg^{167}/Asp^{217} pair), and in the other case, the negatively charged Glu interacts with a His, which could be either neutral or positively charged (His^{299}/Glu^{239} pair).

As shown in Figure 4-I, the subunit (C)His^{299} is in close proximity with subunit (A)Glu^{239} (2.93 Å) and subunit (B)Lys^{245} (3.3 Å). Therefore, any mutation in His^{299} could disrupt all of the interfaces. His^{299} was replaced by Asn, which introduces a neutral residue. Replacing His^{299} by Arg or Lys introduces a positive charge, which could mimic the WT enzyme if His^{299} is positively charged in its native state. However, *all* of the His^{299} mutant enzymes are dissociated into a mixture of species, indicating that in the WT enzyme His^{299} is not positively charged. As modeled *in silico*, the amide group of (C)H299N is further away (3.7 and 5.1 Å) from the side chains of (A)Glu^{239} and (B)Lys^{245} as compared to that of the WT enzyme shown in Figure 4-I. According to the energy-minimized model, introducing a positive charge at position 299 creates both new repulsive and attractive electrostatic interactions (Figure 4-II and -III). For H299R, the electrostatic or H-bonding between (A)Glu^{239} and (C)H299R is maintained while there is a new weak electrostatic attraction between (C)H299R and (B)Glu^{247} and a new repulsive force between (C)H299R and (B)Lys^{245} (Figure 4-II). In the H299K mutant, the Lys side chain is further away from (A)Glu^{239} and gets closer to (A)Glu^{250}, creating a new electrostatic attraction (Figure 4-III). Furthermore, the H299K mutant creates a new repulsive force with (B)Lys^{245} (Figure 4-III). These effects may lead to destabilization of the A/C and B/C subunit interfaces of *all* of the His^{299} mutants, giving rise to mixtures consisting predominantly of monomeric and dimeric species.

In contrast to His^{299} which is shared between the B/C (or A/D) and A/C (or B/D) subunit interface, Glu^{239} is only in the A/C (or B/D) subunit interface. Replacing Glu^{239} with glutamine introduces a neutral polar residue which is

Table 4: Molecular Mass Data and Kinetic Parameters of the *B. subtilis* ASL Mutants of the Arg167/Asp217 Pair

enzyme	AUC data[a] [kDa (%)] tetramer	M−Tet	D−Tet	M−D	gel filtration data[b] (kDa)	$V_{max} \pm$ SE[c] (μmol min^{-1} mg^{-1})	$K_M \pm$ SE[c] (μM)
wild type	205 (100)				216	1.56 ± 0.19	2.6 ± 0.4
R167Q		405 (7)	455 (6)		354	0.01 ± 0.01	13.8 ± 1.4
		72 (93)	105 (94)		89		
R167E				125 (11)	354	*d*	*d*
				68 (89)	89		
					32		
D217N		281 (4)	275 (3)		131	0.02 ± 0.01	41.4 ± 6.5
		72 (96)	97 (97)				

[a] The molecular mass by AUC was measured at 25 °C in 20 mM KPO_4 buffer, pH 7, containing 20 mM KCl using 10K rpm for the mutants of the Arg167/Asp217 pair. [b] The molecular mass by gel filtration was done at 25 °C using a Sephacryl S-200 column equilibrated with 20 mM KPO_4 buffer, pH 7, containing 20 mM KCl. [c] The K_M and V_{max} values were determined by varying the concentration of SAMP and fitting the data to the Michaelis–Menten equation using SigmaPlot. The values are shown along with their standard errors. [d] Not measurable.

comparable in size to glutamate and capable of forming H-bonding with His^{299}. Replacement of Glu^{239} by methionine introduces a neutral nonpolar residue, which does not participate in H-bonding, and by arginine causes a charge reversal at that position. The energy-minimized models show an expanded distance between His^{299} and Met^{239} (5.3 Å) or Arg^{239} (4.8 Å) as compared to the WT distance of 2.9 Å, whereas the distance between His^{299} and Gln^{239} did not change appreciably (3.3 Å). Therefore, E239R and E239M mutant enzymes should destabilize more than the E239Q mutant enzyme. Experimentally, E239R and E239M mutant enzymes exist predominantly as a mixture of monomer–dimer with small amounts of soluble aggregates, and the E239Q mutant enzyme is predominantly composed of monomer–dimer–trimer (Table 3) as predicted by the models. Hence, changing the carboxylate group to an amide group weakens the interaction between the subunit interfaces even though that has the least change in distance. This leads to the conclusion that a carboxylate group at position 239 is important for a complete enzyme assembly and for a fully active enzyme.

The Arg^{167}/Asp^{217} (3.05 Å) pair exists only in the central helical region of the A/C or B/D subunit interface (Figure 5-I) as compared to the His^{299}/Glu^{239} pair which exists on each corner of the A/C or B/D subunit interface. Arginine was replaced with glutamate, to reverse the charge, and each of these residues was replaced with a neutral polar residue, to study the effect of the original charge on the oligomeric structure. As modeled *in silico*, R167E, R167Q, and D217N mutant enzymes do not have charged residues from other subunits in close proximity (Figure 5-II), and the distance increases (>4 Å) between the amino acids at positions 217 and 167 in the mutant enzymes, which could lead to destabilization of the subunit interface. Experimentally, the mutant enzymes of the Arg^{167}/Asp^{217} pair exist predominantly as a mixture of monomer–dimer along with small amounts of aggregates, proving that the increased distance between the subunit interfaces destabilized the enzyme. Furthermore, these results demonstrate that changing the subunit interface residues in the central helical area greatly influences the ASL tetrameric structure.

The V_{max} of *all* of the mutant enzymes are ~1−3% that of the WT enzyme despite their differences in the molecular mass, suggesting that the smaller assemblies are not active and the K_M for SAMP of the mutants increased markedly. Hence, even if the active site of ASL is composed of residues contributed by three or more subunits (*7*), the tetramer form of the enzyme is critical to maintain its full activity. Introducing mutations at the subunit interface disrupts the tetrameric structure, and any decrease in molecular mass results in poor substrate binding, as well as a dramatic decrease in activity.

The deficiency of ASL in humans is due to single point mutations of the gene, which results in autistic features, as well as mild to severe mental retardation, epilepsy, and muscle wasting (*24*). To date, more than 30 point mutations have been identified worldwide (*25, 26*). The majority are located, relatively far away from the active site, in the central

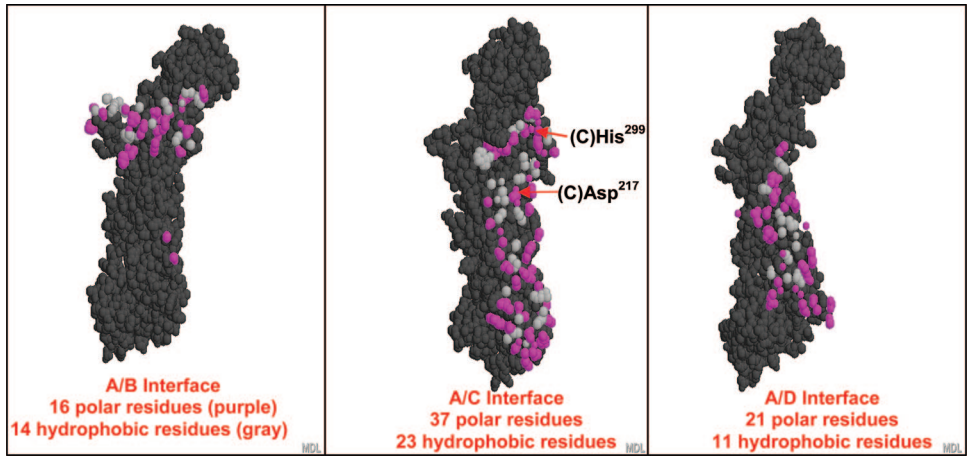

FIGURE 8: Subunit interface residues of B, C, and D subunits which contact the A subunit. Subunit A is shown in dark gray, whereas the polar contact residues of B, C, and D subunits are shown in purple and the hydrophobic contact residues are shown in light gray.

helical region that seems to be important for the stability of the tetramer (*24, 26*). Most of the residues mutated in ASL deficiency are polar (*23–26*), implying that these polar residues are important for the stability of the enzyme. These disease-associated mutations in human ASL could yield enzyme of low activity either by changing the active site or by perturbing the enzyme's multisubunit structure, as shown by our results.

The ASL homotetramer has three different types of interface. The A/B subunit interface has the smallest contact region, whereas the A/C subunit interface has the largest contact region (Figure 1). Taking subunit A as the reference and using the Protein Explorer program, we calculated the number of polar (shown in purple balls) and hydrophobic (shown in light gray balls) residues within 4 Å from the B, C, and D subunits that are in contact with the A subunit (Figure 8). At the A/B, A/C, and A/D subunit interface, 53%, 62%, and 66%, respectively, of the amino acids in the contact region are polar, suggesting that the three types of subunit interface do not contain a unique kind of interaction. Rather, each interface features all types of interactions, and perturbing one type of interaction (hydrophobic or electrostatic) affects all of the subunit interfaces to varying extents. The relatively large contact regions of the A/C and A/D subunit interface are predominantly polar, whereas the contact region of the A/B subunit interface is composed of approximately equal amounts of hydrophobic and polar residues. Given the smaller contact surface between the A and B subunit, if either hydrophobic or electrostatic interactions are weakened, the A/B subunit interface is likely to be the first to be disrupted.

This paper demonstrates that changing polar residues, far from the active site, and perturbing the hydrophobic interactions destabilize the tetrameric form of the enzyme and produce less active enzyme. We conclude that although the majority of the subunit interfaces are composed of a higher number of polar residues than the hydrophobic residues, both types of interactions are important for the stability of the ASL tetramer.

ACKNOWLEDGMENT

We thank Dr. Jennifer L. Hearne for training on analytical ultracentrifugation and Sharmila Sivendran for helpful discussions.

REFERENCES

1. Ratner, S. (1972) Argininosuccinases and adenylosuccinases, in *The Enzymes* (Boyer, P. D., Ed.) 3rd ed., Vol. 7, pp 167–197, Academic Press, New York.
2. Hanson, K. R., and Havir, E. A. (1972) The enzymatic elimination of ammonia, in *The Enzymes* (Boyer, P. D., Ed.) 3rd ed., Vol. 7, pp 75–166, Academic Press, New York.
3. Lee, T. T., Worby, C., Dixon, J. E., and Colman, R. F. (1997) Identification of His^{141} in the active site of *Bacillus subtilis* adenylosuccinate lyase by affinity labeling with 6-(4-bromo-2,3-dioxobutyl)thioadenosine 5′-monophosphate. *J. Biol. Chem. 272*, 458–465.
4. Lee, T. T., Worby, C., Bao, Z., Dixon, J. E., and Colman, R. F. (1998) Implication of His^{68} in the substrate site of *Bacillus subtilis* adenylosuccinate lyase by mutagenesis and affinity labeling with 2-[(4-bromo-2,3-dioxobutyl)thio]adenosine 5′-monophosphate. *Biochemistry 37*, 8481–8489.
5. Lee, T. T., Worby, C., Bao, Z., Dixon, J. E., and Colman, R. F. (1999) His^{68} and His^{141} are critical contributors to the intersubunit catalytic site of adenylosuccinate lyase of *Bacillus subtilis*. *Biochemistry 38*, 22–32.
6. Brosius, J. L., and Colman, R. F. (2000) A key role in catalysis for His^{89} of adenylosuccinate lyase of *Bacillus subtilis*. *Biochemistry 39*, 13336–13343.
7. Brosius, J. L., and Colman, R. F. (2002) Three subunits contribute amino acids to the active site of tetrameric adenylosuccinate lyase: Lys^{268} and Glu^{275} are required. *Biochemistry 41*, 2217–2226.
8. Palenchar, J. B., and Colman, R. F. (2003) Characterization of a mutant *Bacillus subtilis* adenylosuccinate lyase equivalent to a mutant enzyme found in human adenylosuccinate lyase deficiency: Asparagine 276 plays an important structural role. *Biochemistry 42*, 1831–1841.
9. Segall, M. L., and Colman, R. F. (2003) Gln^{212}, Asn^{270}, and Arg^{301} are critical for catalysis by adenylosuccinate lyase. *Biochemistry 43*, 7391–7402.
10. De Zoysa Ariyananda, L., and Colman, R. F. (2007) *FASEB J. 21*, A641.
11. Redinbo, M. R., Eide, S. M., Stone, R. L., Dixon, J. E., and Yeates, T. O. (1996) Crystallization and preliminary structural analysis of *Bacillus subtilis* adenylosuccinate lyase, an enzyme implicated in infantile autism. *Protein Sci. 5*, 786–788.
12. Tornheim, K., and Lowenstein, J. M. (1972) The purine nucleotide cycle: The production of ammonia from aspartate by extracts of rat skeletal muscle. *J. Biol. Chem. 247*, 162–169.
13. Bradford, M. M. (1976) A rapid and sensitive method for the quantitation of microgram quantities of protein utilizing the principle of protein-dye binding. *Anal. Biochem. 72*, 248–254.
14. Hearne, J. L., and Colman, R. F. (2006) Catalytically active monomer of class Mu glutathione transferase from rat. *Biochemistry 45*, 5974–5984.
15. SEDPHAT program Home Page (http://www.analyticalultracentrifugation.com/sedphat/sedphat.htm).
16. Laue, T., Shaw, B. D., Ridgeway, T. M., and Pelletier, S. L. (1992) in *Biochemistry and Polymer Science* (Harding, S. E., Rowe, A., and Horton, J. C., Eds.) pp 90–125, Royal Society of Chemistry, Cambridge, U.K.
17. Toth, E. A., and Yeates, T. O. (2000) The structure of adenylosuccinate lyase, an enzyme with dual acitivity in the de novo purine biosynthesis pathway. *Structure 8*, 163–174.
18. Rodriguez-Zavala, J., and Weiner, H. (2002) Structural aspects of aldehyde dehydrogenase that influence dimer-tetramer formation. *Biochemistry 41*, 8229–8237.
19. Jencks, W. P. (1969) Electrostatic interactions, in *Catalysis in Chemistry and Enzymology* (Hume, D. N., Stork, G., King, E. L., Herschbach, D. R., and Pople, J. A., Eds.) pp 351–392, McGraw-Hill, New York.
20. Oakenfull, D., and Fenwick, D. E. (1977) Thermodynamics and mechanism of hydrophobic interaction. *Aust. J. Chem. 30*, 741–752.
21. Southall, N. T., Dill, K. A., and Haymet, A. D. J. (2002) A view of the hydrophobic effect. *J. Phys. Chem. B 106*, 521–533.
22. Ramos, C. H. I., and Baldwin, R. L. (2002) Sulfate anion stabilization of native ribonuclease A both by anion binding and by Hofmeister effect. *Protein Sci. 11*, 1771–1778.
23. Perez-Jimenez, R., Godoy-Ruiz, R., Ibarra-Molero, B., and Sanchez-Ruiz, J. M. (2004) The efficiency of different salts to screen charge interactions in proteins: a Hofmeister effect? *Biophys. J. 86*, 2414–2429.
24. Van den Berghe, G., and Jaeken, J. (2001) Adenylosuccinate lyase deficiency, in *The Metabolic and Molecular Basis of Inherited Diseases* (Scriver, C. R., Beaudt, A. L., Valle, D., Sly, W. S., Childs, B., Kinzler, K. W., and Vogelstein, B., Eds.) 8th ed., Vol. II, pp 2653–2662, McGraw-Hill, New York.
25. Adenylosuccinate Lyase Mutations Database Home Page (http://www.icp.ucl.ac.be/adsldb/mutations.html).
26. Spiegel, E. K., Colman, R. F., and Patterson, D. (2006) Adenylosuccinate lyase deficiency. *Mol. Genet. Metab. 89*, 19–31.

BI701400C